Critical Review of Vibrational Data and Force Field Constants for Polyethylene

John Barnes and Bruno Fanconi

National Measurement Laboratory, National Bureau of Standards, Washington, D. C. 20234

The results of a critical review of vibrational data, their assignments, and force field constants of polyethylene and the related homologous series of *n*-alkanes are presented. The vibrational frequencies derived from Raman spectroscopy, infrared spectroscopy, and neutron inelastic scattering were collected from the literature. We have reviewed the vibrational band assignments starting from the comprehensive treatment of the *n*-alkanes by Schachtschneider and Snyder [1,2][1] and including subsequent reassignments. Theoretical calculations of the vibrational frequencies were reviewed with emphasis on the various models used for molecular structure and force fields. Lattice dynamical calculations of polyethylene were performed using a valence force field for intramolecular interactions and a force field derived from a nonbonded atom-atom potential function for intermolecular interactions. The molecular and lattice structural parameters were taken from x-ray and neutron diffraction studies of polyethylene and selected *n*-alkanes. A refinement procedure was carried out by the method of least squares on intramolecular force field constants and on parameters of a phenomenological nonbonded atom-atom potential energy function. The resulting force field constants and associated standard deviations are presented.

Keywords: Force field refinement; lattice dynamics; *n*-alkanes; non-bonded potential functions; polyethylene; vibrational data.

1. Introduction

Polyethylene is the simplest synthetic polymer in terms of chemical composition and has been extensively studied through a variety of techniques. Not only is it an important commercial polymer, but also its chemical simplicity and the availability of well-characterized oligomers which are chemically and structurally equivalent make polyethylene an ideal model system for other polymers.

In this report, we review one aspect of the characterization of polyethylene, viz., the interpretation of its vibrational spectra and concomitantly those of the *n*-alkanes. Vibrational data have been derived from infrared, Raman and inelastic neutron scattering spectroscopies with the most recent data coming from neutron and Raman scattering measurements. We critically review these data with regards to accuracy, physical state of the sample, and temperature of measurement.

Theoretical vibrational frequencies have been calculated assuming various models of the molecular structure and force fields. These calculations assume band assignments which have undergone considerable revision as new experimental data became available. We have reviewed the vibrational band assignments starting from the comprehensive treatment of the *n*-alkanes by Schachtschneider and Snyder [1,2] and including subsequent reassignments.

The most recent vibrational data concerns the low frequency vibrations which involve lattice vibrations or combinations of lattice vibrations with low frequency internal skeletal deformation motions. The involvement of intermolecular vibrations implies that the frequencies of these vibrations are strongly influenced by intermolecular interactions and hence may be used to test phenomenological potential energy functions used to describe nonbonded atom-atom interactions. Although calculations have been carried out utilizing some of these recent data with simplified models of the nonbonded interactions there has not been a systematic study which includes the higher frequency data in the analysis. We have performed lattice dynamical calculations of polyethylene using a general force field for intramolecular interactions and a force field derived from nonbonded atom-atom potential functions for intermolecular interactions.

In subsequent sections, we review the structural data, vibrational data, assignments of the vibrational data, previous theoretical calculations and the results of our lattice dynamical calculation.

2. Structural Data

2.1. General Structural Features of Polyethylene

The structure of polyethylene [3-6] is intermediate between a perfectly ordered crystalline solid and an amorphous one. Electron microscopy has shown [6] that polyethylene crystallized from dilute solution exhibits regions of high crystallinity in which the main structural features are chain-folded lamellae and amorphous or disordered regions comprising the chain folds and interlamellar spaces. The volume fraction crystallinity [7-10] depends significantly on the method of sample preparation and under favorable conditions may approach 80% crystallinity [6].

[1] Figures in brackets indicate the literature references at the end of this paper.

A number of spectral features in infrared, Raman and neutron scattering data are sensitive to the degree of crystallinity [11-14]. Although it is relatively straight-forward to separate crystalline spectral features from amorphous ones, there remains the problem of the effect on the spectra due to the perturbation of the crystalline core by the amorphous region. Fortunately, most of the spectral data used in the vibrational analysis derives from the normal alkanes which are short chain counterparts of polyethylene. The normal solid state of the *n*-alkanes is entirely crystalline and questions of the influence of noncrystalline regions do not enter. The terminal methyl groups of the *n*-alkanes can give rise to spectral features which must be accounted for in the data analysis. In what follows, we shall consider only crystalline polyethylene and references to polyethylene will implicitly mean a perfectly crystalline material.

The main assumption in the use of *n*-alkane vibrational data to predict vibrational properties of polyethylene is that the oligomer and polymer be structurally isomorphic. That is, the molecular geometry (bond lengths, bond angles, and internal rotation angles) and the arrangement of methylene units in the lattice should be identical. Structural determinations [3, 15-22] have demonstrated that the molecular geometry is nearly identical in polyethylene and the *n*-alkanes although there are slight variations in bond distances near the chain end in the *n*-alkanes. For crystalline *n*-alkanes longer than *n*-pentane, it has been found [15-22] that the chain axes are parallel as in polyethylene; however, the lateral packing of the chains differ in some *n*-alkanes from that found in polyethylene. It has been observed that the vibrational spectra, especially in the low frequency regions, strongly depend on the lateral packing.

2.2. Crystalline Polyethylene

Polyethylene crystallizes with two chains in the Bravais unit cell, each of which contributes two methylene groups of the four comprising the orthorhombic unit cell. The space group is P_{nam} which is isomorphic to the point group D_{2h}. The molecular planes of the two chains in the unit cell make an angle with respect to the lateral unit cell directions which defines the setting angle. In the literature, one finds the setting angle defined with respect to both the a and b crystallographic axes. We define the angle with respect to the *a* or long axis.

Temperature dependent studies of lattice parameters and to a lesser extent setting angle have been reported [4, 23-29]. We chose values from a neutron diffraction study of perdeuteropolyethylene [29] since the measurement temperature (90 K) was near to that of most spectroscopic data used in the vibrational analysis. The value of the setting angle greatly influences frequencies associated with factor group splittings and lattice modes. It is found that the value of 41° from neutron diffraction yields better overall agreement between theoretical and experimental frequencies taken at temperatures near 90 K than does 48° which is the generally accepted room temperature value. Snyder [30] has estimated a value of 42° for 93 K from an analysis of the infrared intensities of the methylene rocking components. The molecular geometry and lattice parameters are summarized in table 1.

TABLE 1. Molecular and crystallographic structural parameters of polyethylene

Molecular structure[a]	
C-C	0.1532 nm
C-H	0.1058 nm
C-C-C	112.01°
HCH	109.29°
Orthorhombic lattice parameters[b]	
$a = 0.7161$ nm, $b = 0.4866$ nm, $c = 0.25412$ nm, $\Phi = 41°$	
Triclinic[a]	
$a = 0.422$ nm, $b = 0.479$, $c = 0.25412$ nm, $\alpha = 89.545°$, $\beta = 71.497°$ nm, $c = 0.25412$ nm, $\alpha = 89.545°$,	

[a] H. Mathisen, N. Norman, and B. F. Pedersen, Acta Chem. Scand. 21, 127-135 (1967).
[b] G. Avitabile, R. Napolitano, B. Pirozzi, K. D. Rouse, M. W. Thomas, and B. T. M. Willis, J. Poly. Sci. B 13, 351 (1975).

2.3. *n*-Alkanes

The various crystal structures of the *n*-alkanes will be reviewed. The literature referred to is fairly recent; older references can be found in a review by Broadhurst [31]. The pure *n*-alkanes crystallize in different lattice structures depending on chain length, parity of the number of carbon atoms, and the temperature. The two main crystallographic classes are the triclinic form, containing one molecule per unit cell, exhibited by the even alkanes between *n*-C_6H_{14} and *n*-$C_{26}H_{54}$ and the orthorhombic form, containing four molecules per unit cell, characteristic of the odd *n*-alkanes above *n*-$C_{11}H_{24}$ and the longer even alkanes. The local arrangement of the methylene groups also constitutes a unit cell referred to as the subcell. For the triclinic structure [19-22] the subcell is also triclinic containing two methylene groups of the single chain in the unit cell. The orthorhombic structure [15, 16, 18] has a subcell identical to that of polyethylene.

Detailed structural analyses have been carried out on *n*-hexane [20], *n*-octane [19, 21], and *n*-octadecane [22] among the triclinic modification. The most complete determination has been that of *n*-octane. The other determinations are in substantial agreement and it is concluded that the other members of the series are isostructural.

The even-numbered *n*-alkanes above *n*-$C_{24}H_{50}$ may also exhibit monoclinic modifications [16, 31, 32] in which the subcell remains orthorhombic and polyethylene-like. The two chain molecules in the macrocell are arranged in a layer structure in which the chain axes are inclined with respect to the layer planes. Different degrees of inclination have been observed with staggering of the chain equivalent methylene groups along different crystallographic directions. The manifestations of monoclinic modification on infrared and Raman spectra will be discussed.

The orthorhombic unit cell of the *n*-alkanes contains four molecules, two in each of two layers [15, 18]. The chain axes are perpendicular to the planes of the terminal methyl groups. In addition to these structures, there exists, in some *n*-alkanes, a hexagonal structure a few degrees below the melting point [25]. Although the details of this structure have not been determined, it is evident that the molecular chains are perpendicular to the end group plane [24], that they have rotational freedom about their long axis [26-30], and that there is one molecule per unit cell. The hexagonal structure has been observed in the odd *n*-alkanes from *n*-$C_{19}H_{40}$ to *n*-$C_{43}H_{88}$ and in the even *n*-alkanes *n*-$C_{22}H_{46}$ to *n*-$C_{44}H_{90}$.

The analysis of *n*-alkane structures shows that there are two prominent lateral packing or subcell geometries; in one, the unit cell is triclinic containing a single chain, and in the other, the unit cell is orthorhombic containing two chains as in polyethylene. In our calculations, to be discussed in detail in section 4, the full utilization the vibrational data of the *n*-alkanes required that two separate lattice structures be used for polyethylene, one was the usual orthorhombic cell, and the second was based on the triclinic subcell. These two structures were used to set up two separate lattice dynamical calculations using a common intramolecular valence force field and intermolecular potential energy function.

The use of a common intramolecular force field required that a common molecular geometry be used for both structures. The bond lengths and bond angles of such a structure were derived from x-ray data on *n*-octane [21] by obtaining the best fit to atomic positions, using one value for all C-C bond distances, another for all C-H bond distances and likewise for the HCC, HCH, and CCC angles. The values of the CC and CH bond lengths and the CCC and HCH angles are shown in table 1 along with the lattice parameter data.

3. Vibrational Data and Assignments

3.1. Infinite Chain Lattice Approach

Vibrational data were compiled from infrared [39-54], Raman [55-57], and neutron scattering [78-89] spectroscopic studies on polyethylene and selected *n*-alkanes. Infrared and Raman data from the literature prior to 1963 have been used by Schachtschneider and Snyder [1,2] to arrive at force fields suitable for isolated chain models. We shall review only the more recent data which is comprised mainly of low frequency infrared spectra, Raman spectra, and inelastic neutron scattering results. These data are extremely important in characterizing low frequency motions as well as the influence of the lattice on these motions and on the correlation or factor group splitting of higher frequency intramolecular modes. Factor group splittings which are well known in infrared spectra have been observed in recent Raman studies [61,66,72,74].

For an isolated transplanar polyethylene one would expect [90] only transverse and longitudinal acoustic vibrations below 550 cm^{-1}. These modes are comprised of deformations of skeletal atoms both in and out of the molecular plane and involve internal coordinates of the CC stretch, CCC angle deformation, and torsion. The large frequency gap between skeletal modes and methylene modes (150 cm^{-1}) implies that coupling between them is minimal and, hence, band assignments are somewhat simplified.

In crystalline polyethylene the lattice interactions modify the transverse and longitudinal acoustic vibrations of the two chains in the unit cell to produce lattice vibrations which at the Brillouin zone center are termed lattice modes. There are a total of eight lattice modes in polyethylene of which three have zero frequency. From group theory it can be shown [91] that the five non-zero frequency lattice modes comprise two Raman-active librational modes, two infrared-active translatory modes, and one spectroscopically inactive translatory mode.

The lattice modes of the *n*-alkanes are described in terms of the macrocell geometry as motions involving entire molecules. A correspondence to polyethylene lattice modes may be made through the subcell geometry. The triclinic *n*-alkanes are the simplest since there is a single molecule in the macrocell [21] and a total of six lattice modes. Three have zero frequency and correspond to the three pure translations of the subcell lattice. The remaining three are the long axis librational mode which corresponds to the single librational lattice mode of the triclinic subcell lattice, and two librations about axis perpendicular to the molecular axis which correspond to zone interior modes of the subcell lattice. The latter two modes may be described as transverse acoustical vibrations of the triclinic infinite chain lattice [69].

The orthorhombic *n*-alkanes have four molecules in the macrocell [15] and a total of 24 lattice modes. For each of the eight lattice modes of the orthorhombic subcell one may construct a symmetric and antisymmetric lattice mode of the double layer structure using one component from each of the two layers. Of the 16 modes thus formed, three represent pure translations (symmetric combinations of polyethylene translations), ten are the symmetric and antisymmetric combinations of non-zero frequency lattice modes of polyethylene, and three are new translatory modes corresponding to relative displacements of the two layers with respect to each other. The remaining eight modes (24-16) are combinations of librations about axes perpendicular to the chain axis and have no anologs at the zone center in polyethylene but correspond to zone interior modes of a predictable phase value dependent on the *n*-alkane's chain length [69, 71].

Due to the weak coupling between layers, it is expected [67, 69] that the frequencies of the combinations of the five non-zero frequency lattice modes would be nearly identical to those of polyethylene. The general use of low frequency *n*-alkane data to describe vibrations of the infinite chain lattice will be discussed in more detail in section 4.

3.2. Far Infrared Data[2]

Two bands have been observed in the far infrared spectrum of polyethylene [43-49,51-54], at 73 and 94 cm^{-1} at 298 K, and at 80 and 109 cm^{-1} at 2 K. The lowest frequency band of the pair was attributed [44,45] to the crystalline phase since the band intensity increased with increasing

[2] Following the practice customary in this field, vibrational frequencies are expressed in wavenumber equivalents (cm^{-1}), i.e., frequency divided by the speed of light.

volume fraction crystallinity. The temperature dependence [44,47] and intensity [44] were indicative of crystalline lattice modes. The assignment to an infrared-active translatory mode was substantiated by deuteration experiments [47], the presence of the band in orthorhombic but not in triclinic *n*-alkanes [47], and polarization studies [49].

Theory predicts two infrared-active lattice modes in polyethylene. The higher frequency band is extremely weak and was initially observed [48] only at low temperatures. Subsequent measurements [53,54] at higher signal-to-noise enabled location of the band at 94 cm^{-1} at room temperature. The assignment of this band to the B_{2u} lattice mode was based on its appearance in the spectrum of orthorhombic *n*-alkanes [48] and the excellent agreement with the theoretical frequency.

3.3. Raman Spectra

The initial observations of low frequency Raman bands in the *n*-alkanes was reported by Simanouti and Mizushima [55] and later in more detail by Schaufele and Shimanouchi [57]. A series of bands was observed for each *n*-alkane in the solid state which were assigned to longitudinal acoustical vibrations from the frequency dependence on chain length, and the similarity between the derived Young's modulus and that of diamond. Studies [69, 74] on an extensive series of *n*-alkanes using special experimental techniques to obtain extremely low frequency data have yielded frequencies assignable to lattice modes and to transverse acoustical branches. The results pertain both to orthorhombic and triclinic crystalline modifications. As would be expected, the spectra are greatly influenced by the lateral packing of the *n*-alkane chains; the spectra of triclinic *n*-alkanes which contain one chain per subcell are less complex than those of orthorhombic *n*-alkanes which contain two chains in the subcell.

Tentative assignments have been advanced on the basis of existing lattice dynamical calculations by several independent groups of investigators [69, 71, 73]. In addition to the extensive study referenced above, there have been limited studies on selected *n*-alkanes [67, 71, 75]. It has been observed [68] that crystalline polymorphism in terms of how the *n*-alkane molecules pack in the lattice can lead to substantial differences in the vibration pattern. Two explanations have been advanced [68, 77] to explain the frequency shifts. One arises from the symmetry requirements for spectroscopic activity. The in-phase relationship of translationally equivalent displacements implies that the active modes of the subcell lattice correspond to a wavevector which varies according to the details of the molecular packing. Another cause for the observed frequency differences may be the influence of the methyl group packing, and small frequency shifts of the longitudinal acoustic mode associated with polymorphism have been attributed to this effect. We have shown from lattice dynamical calculations of *n*-octane that the frequency of the short axis librational modes are nearly identical to those calculated from the infinite triclinic polymer crystal, and hence not influenced by the methyl group packing.

Conflicting assignments have been advanced [73, 75] for the long axis librational mode in triclinic *n*-alkanes. Recent studies [76] on deuterated *n*-alkanes have established that the frequency of this mode lies near 60 cm^{-1} in contrast with calculated values of 100 cm^{-1}. One calculation of 49 cm^{-1} for this mode in *n*-octane [75] appears to be in error as a result of misassigning the calculated frequency. We have duplicated this calculation and found the the highest frequency librational mode corresponds to long axis rotation and not to one of the two short axis librational modes as previously reported [75].

The two Raman-active lattice modes of polyethylene have been observed [70] at low temperature and assigned from polarization studies as shown in table 2. Studies with *n*-$C_{36}D_{74}$ have confirmed [76] the assignments.

New Raman data in the region of the methylene deformations and optical skeletal modes have also appeared [61]. These data relate to the assignment of the methylene wagging fundamental and to factor group splittings. The initial assignment of the B_{2g} methylene wagging fundamental to the Raman band at 1415 cm^{-1} was questioned by Snyder [60, 92] from infrared studies of *n*-alkanes in the melt and α, ω-dichloro-alkanes in the solid state. Snyder proposed [92] a frequency limit of 1382 cm^{-1} for the methylene wagging branch from the infrared results and suggested that the 1415 cm^{-1} band was due to a combination or overtone band involving the rocking modes. Although the earlier Raman studies of polyethylene were unable to locate a band near 1375 cm^{-1} more recent studies [60, 62, 65] have revealed a band at 1370 cm^{-1} with polarization characteristics consistent with those of the wagging fundamental.

Other recent Raman studies [62, 63, 65, 66] in the mid-frequency range have focused on polarization data to substantiate assignments of fundamental, combination, and overtone modes. Low temperature studies [61] at high resolution have resolved the factor group splittings of the methylene twisting and optical skeletal modes. Raman studies at elevated pressures [66, 72, 74] reveal additional structure in the methylene bending region which is assigned to Fermi resonance between overtones of the methylene rocking fundamental and the bending fundamental. From pressure studies [72] it was concluded that Fermi resonance interactions result from intermolecular anharmonicity.

Another assignment for the 1415 cm^{-1} band is to a factor group component of the methylene bending vibration

TABLE 2. Lattice Modes of *n*-alkanes and polyethylene

Type	Symmetry	Frequencies (cm^{-1}) obs.	calc.
Orthorhombic structure			
librational	A_g	136	141
translatory	A_u	inactive	55
translatory	B_{1u}	81	86
translatory	B_{2u}	106	109
librational	B_{3g}	108	102
Triclinic structure			
librational	A_g	60	63

[61]. This band disappears in the triclinic and hexagonal rotator phase which would indicate that it is factor group splitting component. However, the methylene rocking region only shows a single band in these modifications so that rocking combination bands are no longer possible likewise. The symmetry of the 1415 cm^{-1} band is A_g [65] in agreement with the calculations of the lower frequency factor group component of the methylene bending vibration. However, an analysis [92] of the Fermi resonance possibilities yields a combination band of A_g symmetry. It is concluded that the assignment of the 1415 cm^{-1} band remains unresolved at this time.

3.4. Neutron Scattering

The frequency range accessible in inelastic neutron scattering experiments is between 25 cm^{-1} and 800 cm^{-1} with the major part of the data coming between 50-600 cm^{-1}. In polyethylene, maxima in the vibrational density of states derived from incoherent neutron scattering correspond to the frequency maxima of the longitudinal and acoustical branches and the five zone center lattice modes. At higher frequencies are found scattering maxima which may correspond to multiphonon events, but the lower frequency events are undoubtedly related to singularities in the density of states at the zone center.

In hydrogeneous polyethylene prominent maxima in the density of states are found [79] near 200 and 550 cm^{-1}. Studies [82, 84, 85] on stretched, uniaxially oriented samples have shown that the maximum at 550 cm^{-1} is associated with longitudinal motion as would be the situation for longitudinal acoustical vibrations and that the maximum at 200 cm^{-1} is associated with transverse motion although the persistence of transverse response is unexpectedly large in the longitudinal experiment.

The frequency limit of the longitudinal acoustic branch ν_5 was found [82] to be 525 ± 15 cm^{-1} at 100 K and in another experiment [85] to be no higher than 536 cm^{-1} at a measurement temperature of 4.2 K. An event near 50 cm^{-1} cannot be attributed to the c axis translatory lattice mode since the structure factor should be zero for out-of-phase motion. Analysis of the phonon dispersion of all wavevectors in the Brillouin zone, based on a simplified model involving only four different intermolecular interactions, has shown [93, 94] that weak maxima may arise from non-zone center modes.

A feature in the inelastic neutron scattering spectrum at 240 cm^{-1} has been attributed [83, 84, 93] to either the maximum of one of the transverse acoustical (TA) branches or to a multiphonon mode. A difficulty in the assignment is the persistence in the longitudinal spectrum of the feature at 190 cm^{-1} suggesting that this event may be due to multiphonon effects. Other work [87] on extended chain polyethylene with regard to polarization and temperature dependence has established the cutoff frequencies of the two TA branches at 193 and 214 cm^{-1}.

The dispersion of the longitudinal skeletal vibrations was measured [86] directly by coherent neutron scattering from perdeuterated polyethylene. The maximum of the longitudinal acoustic branch occurs at 453 cm^{-1} which agrees with the result obtained from incoherent scattering from normal polyethylene when the frequency is corrected for the mass difference. A portion of one TA branch near the zone center has also been detected by coherent scattering. It has been shown [95] that the structure factors of the TA modes are vanishingly small except near the zone center. The portions of the TA and LA branches determined by coherent neutron scattering are in substantial agreement with those found from analysis of the Raman data.

4. Calculations of Normal Modes of Vibration

4.1. Polymeric Crystals

The total number of vibrational frequencies of a crystal containing N atoms will be $3N$ of which a small subset, $3n$, equal to the number of cartesian displacements within the Bravais unit cell may be spectroscopically active. The frequencies fall on a set of three-dimensional surfaces with the number of surfaces equal to $3n$. A particular frequency may be labeled by the surface to which it belongs and a wavevector in the first Brillouin zone. The wavevector is a reciprocal lattice vector, the components of which give the phase relation along three mutually perpendicular directions. At each wavevector, there will be $3n$ modes; the spectroscopically active modes occur at wavevector equal to zero [96, 97] termed the zone center of the Brillouin zone.

The polymeric crystal differs from the nonionic small molecule crystal in that the forces along the chain axis crystalline direction are valence forces and hence much stronger than the usual nonbonded van der Waals forces between molecules in the solid state. The anisotropy of forces means that the number of lattice modes at the zone center is reduced by a factor of a third for the polymeric crystal.

The unit cell of polyethylene contains two chains and each chain contributes two methylene units to the total of four methylene groups in the unit cell. The number of cartesian displacements equals 36 and a projection of the frequency surfaces along a wavevector direction corresponding to the chain axis will contain 36 curves comprised of the following descriptions starting from the lowest frequency branches: 2 transverse acoustical, longitudinal acoustical, 9 skeletal optical, 4 methylene rock, 4 methylene wag, 4 methylene twist, 4 methylene bend, 4 CH_2 symmetrical stretch, and 4 CH_2 asymmetrical stretch.

The spectroscopically active vibrations of crystalline polyethylene correspond to zero phase value. An analysis [97] of the unit cell symmetry isomorphic to the space group, D_{2h}, shows that 15 vibrations are active in the infrared, 18 in the Raman and 3, the A_u vibrations, are inactive in both the infrared and Raman.

The finite length of an oligomer gives it a special property in comparison to the polymer. In the crystal of the oligomer the spectroscopic selection rule is given by the $k = 0$ conditions where the wavevector is of the macrocell Brillouin zone. The macrocell is the unit cell containing as entities entire oligomeric molecules. All internal vibrations of the oligomeric molecule are permitted by the $k = 0$ selection rule; however, the symmetry of the molecule itself may forbid certain modes from being either infrared or Raman-

active. The internal vibrations in the absence of end groups effects are identical to subcell vibrations and may be specified by subcell wavevectors which are integral multiples of the reciprocal oligomeric length.

It is possible, therefore, to map out the phonon dispersion curves (frequency versus wavevector) of the polymer from spectral data of a series of molecules isostructural to the polymer [98]. The oligomeric data are classified according to the subcell wavevector and frequency surface. The larger values of the wavevector sampled through the use of oligomeric data come from the shorter oligomers where end group effects may be important. It has been experimentally observed [69, 98] that the band intensities decrease with increasing subcell wavevector values, and for the same wavevector value with increasing oligomeric length. When the oligomers become exceedingly long, the spectra approach that of the polymer.

4.2. Review of *n*-Alkane and Polyethylene Calculations

Vibrational force fields for polyethylene have evolved through consideration of vibrational frequencies of the polymer and its oligomers, the *n*-alkanes. The first extensive treatment of vibrational spectroscopic data of *n*-alkanes was carried out by Schachtschneider and Snyder [1,2] who used data, mainly infrared, from a large number of *n*-alkanes to derive by least squares refinement procedures several force fields of the valence and Urey-Bradley [99,100] type. The overall agreement with experimental frequencies obtained from valence force fields was superior to that obtained from the Urey-Bradley field. The *n*-alkanes were treated as isolated molecules in the extended transplanar conformation of the solid state. A subsequent treatment [101] of *n*-alkanes in non-planar conformations has been carried out. In the original Schachtschneider and Snyder [1,2] treatment the B_{2g} methylene wagging fundamental of polyethylene was misassigned to a Raman band at 1415 cm^{-1}. Subsequent analyses [60,92] have shown that the wagging fundamental should be assigned to a Raman band at 1375 cm^{-1} and the valence force field was modified slightly to account for the change in assignment.

Calculations of the vibrational frequencies of polyethylene have utilized models of the structure and force fields of varying degrees of completeness. Initially, simple dynamical models were used to predict [102] the behavior of skeletal vibrations and the intermolecular effects [103-105] on localized methylene vibrations. Calculations [90] in which the methylene group was treated as a single dynamical entity yielded dispersion curves which were found not to closely approximate experimental curves due to the complete neglect of coupling between skeletal vibration and high frequency intramolecular vibrations. An improved description [106-110] of the dispersion curves resulted from explicit treatment of methylene hydrogens using an isolated transplanar chain model. However, interchain effects on the intramolecular vibrations are necessarily not considered with the isolated chain model, and in addition, there is no treatment of lattice vibrations.

The lattice influence on intramolecular modes may be to shift the frequencies slightly and to split a mode into two or more components. The number of components is equal to the number of molecules in the unit cell and the process is referred to as Davydov or factor group splitting. The isolated molecule model involves the assumption that the effect of intermolecular interactions on intramolecular vibrations can be approximated by adjustments of the intramolecular force constants. Since the experimental data are derived from measurements in the condensed phase force fields derived from isolated chain calculations necessarily include lattice interactions, although details such as factor group splittings and lattice modes cannot be accounted for in the model.

Using the assumption that methylene units may be treated as single dynamical units for the purpose of calculating lattice vibrations, several groups of investigators have calculated [111-115] the dispersion of the lattice modes. Reasonable agreement with the translatory lattice modes was obtained [90,112] using a model in which only the interchain interactions corresponding to the three or four shortest carbon-carbon distances were taken to be non-zero. The agreement with the librational lattice frequencies of polyethylene was poor, reflecting the importance of the hydrogen atom locations. The pendant hydrogen atoms undergo large displacement amplitudes in librational motion. Even though the agreement with spectroscopic frequencies is approximate, the skeletal model has been useful [90,115] in calculating the density of vibrational states in the low frequency range. The density of states has compared favorably to inelastic neutron scattering results especially when estimates of scattering amplitudes are included in the analysis [113].

Lattice dynamic calculations of the polyethylene lattice have been reported by numerous groups [61,67,70,111,115-118] however, the only detailed accounts are those of Tasumi and Shimanouchi (TS) [117] and Tasumi and Krimm (TK) [118]. The calculation of TS started with the isolated chain force field developed by Tasumi et al. [107] and included the lattice interactions. The interchain force field used by TS consisted of only hydrogen-hydrogen interactions and only the four shortest H . . . H distances were considered to have nonzero interactions. Each H . . . H interaction was treated as a bond stretch which is equivalent to neglecting the linear term (first derivative of the potential function with respect to the interatomic distance) in transforming the derivatives of the potential function to cartesian coordinates. Three of the four force constants were adjusted to match observed ir splittings of the methylene rocking and bending modes and the infrared active B_{1u} translatory mode. The other interaction constant did not influence the observed splittings and lattice frequencies and was given a value estimated from the other three. Although the four values do not correspond to values derivable from a common potential function they do monotonically decrease with increasing hydrogen-hydrogen distances, and are of the proper magnitude. Further work carried out by Tasumi and Krimm [118] included an investigation of dipole-dipole interactions, an attempt to derive the interaction constants from a common potential function, and consideration of the effects of temperature on the frquencies through changes in lattice parameters and setting angle. It was found that the dipole-dipole term did not contribute substantially. Force field constants

taken from the earlier calculation were modified to account for nontetrahedral geometry.

Two lattice dynamical calculations of triclinic *n*-alkanes have recently been reported.[73,75] These calculations have utilized interchain force constants derived from nonbonded potential energy functions to assign lattice and low frequency intramolecular modes of vibration. The overall agreement between the calculated and experimental frequencies is reasonable as is the agreement between the two calculations with the exception of the assignment of the long axis librational mode in *n*-octane. Brunel and Dows [75] have calculated the long axis librational mode frequency at 49 cm^{-1} whereas Takeuchi et al. [73] calculate a frequency of 101 cm^{-1}. Both calculations used the same structural data for *n*-octane and the same nonbonded potential energy function although there were differences in the interaction summation radii and also in the treatment of linear terms arising from differentiation of the potential function to arrive at force constants.

4.3. Lattice Dynamical Calculation

The survey of spectral data and calculations of polyethylene has demonstrated the need for a lattice dynamical calculation which encompasses recent structural and vibrational data.

The assignment of the Raman-active methylene wagging fundamental has been resolved [60], however, the assignment of the Raman band at 1415 cm^{-1} remains inconclusive. The agreement between band frequencies of the Raman-active librational modes and the calculated values has been mediocre. Low temperature Raman studies [76] of *n*-alkanes and selected deuterated *n*-alkanes have confirmed the assignments of librational lattice modes of orthorhombic polyethylene, and have shown that a band near 60 cm^{-1} may be assigned to the long axis librational mode of triclinic *n*-alkanes. The long axis librational mode of orthorhombic *n*-alkanes and polyethylene with in-phase relationship between the two chains in the unit cell has an experimentally determined [70] frequency of 110 cm^{-1}. This frequency is considerably higher than the value for the similar type motion of triclinic *n*-alkanes (60 cm^{-1}); to fit both of these values with a intermolecular force field derived from the same nonbonded potential energy function provides a stringent test of this function.

We have carried out a refinement by the method of least squares starting from the general force field of Tasumi and Shimanouchi [105]

$$V = \frac{1}{2} \sum_{hkl} \sum_{h'k'l'} \sum_{ij} f_{ij}^{hkl,h'k'l'} S_i^{hkl} S_j^{h'k'l'},$$

where the first two summations are over the unit cells, the third summation is over the local symmetry coordinates within the unit cells, and $f^{hkl,h'k'l'}$ is the second derivative with respect to local symmetry coordinates S^{hkl} and $S^{h'k'l'}$.

Local symmetry coordinates of the type methylene rock, twist, wag and bend and C-H symmetric and asymmetric stretch, defined in table 3, were used in the calculation. The benefit of localized symmetry coordinates is to remove the redundant bending coordinate about the carbon atom and thereby to minimize correlation among valence force constants. In the initial valence force field we included all interactions between coordinates involving at least one common atom. All values were initialized to the values of Tasumi and Shimanouchi [117]. In the refinement procedure the valence

TABLE 3. Definition of localized symmetry coordinates

Symmetry Coordinates	Internal Coordinates							
Symmetric CH_2 stretch	$1/\sqrt{2}$	$1/\sqrt{2}$						
Antisymmetric CH_2 stretch	$1/\sqrt{2}$	$-1/\sqrt{2}$						
Skeletal angle bend			a	$-b$	$-c$	$-c$	$-c$	$-c$
CH_2 bend				d	$-e$	$-e$	$-e$	$-e$
CH_2 wag					f	f	$-f$	$-f$
CH_2 rock					f	$-f$	f	$-f$
CH_2 twist					f	$-f$	$-f$	f
	CH bond stretch	CH′ bond stretch	C_-CC_+ angle bend	HCH′ angle bend	C_-CH angle bend	C_-CH' angle bend	C_+CH angle bend	C_+CH' angle bend

$a = 0.909633$, $b = 0.180325$, $c = 0.187116$
$d = 0.900871$, $e = 0.217044$, $f = 0.5$

force constants separated into two sets, one involving methylene rock, methylene twist, skeletal torsion and asymmetric C-H stretch, and the second involving methylene wag, methylene bend, C-H symmetric stretch, skeletal stretch and angle deformation. We carried out the refinement process separately for each of the two sets of force constant parameters including those experimental frequencies from both triclinic and orthorhombic lattice structures which depend on the force constant set considered. To fully utilize the vibrational data of the *n*-alkanes, especially low frequency data, we have used two different subcell geometries for the force field refinement. One was the usual orthorhombic lattice of polyethylene and the second was the triclinic subcell geometry of the even *n*-alkanes. The method of selecting the molecular and subcell lattice parameters have been discussed and the values given in table 1.

Sources of the vibrational data used in the analysis are: infrared, ref. 39-54; Raman, ref. 55-77; and neutron scattering, ref. 78-89. Where possible, we have collected data taken at similar temperatures near 90 K, the temperature of the neutron diffraction study [29] from which we have taken values of the orthorhombic lattice parameters and setting angle. The vibrational frequencies and their assigned phase values were collected according to dispersion curves. In this manner, experimental dispersion curves along the chain axis direction were determined. For each of the polyethylene dispersion curves, except those associated with C-H bond stretch, a statistical analysis was used to determine the most probable frequencies at selected values of the phase used in the calculation. The phase values chosen were 0, 0.25, 0.5, 0.75, and 1.0 in units of $\pi/2.5412$ Å^{-1}. After preliminary calculations we were able to unambiguously assign additional IR bands of the *n*-alkanes for which previous assignment of phase values were not possible. In total, 705 frequencies were used in the analysis including infrared, Raman, and coherent neutron scattering data from perdeuteropolyethylene.

There was no appreciable correlation between the two sets of parameters but significant correlation between some parameters within a set. When two or more parameters are highly correlated it is not meaningful to carry out a linear regression analysis in the usual way. Our procedure was to transform the parameter set using the variance-covariance matrix to an independent set and perform the linear regression on the transformed parameter set. In this manner we were able to estimate by the back transformation which of a set of highly correlated parameters were most significant in reducing the sum of least squares. The most significant parameters by this procedure were included in the refinement procedure.

For the intermolecular interactions we started from the Williams' IV [108] potential which has the form

$$V(r) = A/r^6 + Be^{-Cr},$$

in which r is the distance between atoms on different molecules and there is a different set of parameters A, B, and C for each of the interaction types, H . . . H, H . . . C, and C . . . C. Williams fitted [108] the A and B parameter values by weighted least squares from sublimation energies, elastic constants, and crystallographic structural data. The A parameter value for C . . . H interactions was taken as the geometric mean of the H . . . H and C . . . C values. The C values for H . . . H and C . . . C were estimated from quantum mechanical calculations of repulsion between two hydrogen molecules and from the interplanar spacing and compressibility of graphite, respectively. The C value for H . . . C was taken as the mean value for H . . . H and C . . . C. The C values of Williams were retained in our treatment and we refined on the A and B parameter values treating correlation between parameters in the manner described above.

The elements in the dynamical matrix for nonbonded interactions are found by differentiating the nonbonded potential energy term with respect to cartesian coordinates. This procedure generates both first and second derivatives of the potential function referred to as linear and quadratic terms, respectively. Some earlier lattice calculations [117-118] have ignored the linear term by assuming that all interaction distances correspond to the minimum in $V(r)$. An analysis of the distances between atoms belonging to different molecules in the crystal structure shows that this is not the case and that the linear term can be appreciable for distances in the repulsive part of the potential.

We have analyzed the effect of the linear term on the lattice frequencies and found that the major influence was on the librational lattice frequencies. This analysis shows why the previously calculated [117-118] librational lattice frequencies were too large while the translatory frequencies agreed well with experimental values.

The final set of general force field parameters with standard deviations are shown in table 4, and the nonbonded potential function values are given in table 5. The agreement with experimental frequency is indicated by comparisons of dispersion curves shown in figures 1-6 and Brillouin zone center frequencies in table 6. The agreement is excellent (2.5 cm^{-1}) with the largest discrepancies involving the transverse acoustical branches shown in figures 5 and 6. Within the model used in the calculation we were able to achieve better agreement in the transverse acoustical branches without sacrificing the excellent agreement of zone center lattice modes.

One possible source of the disagreement between calculated and experimental transverse acoustic vibrations may be the terminal methyl groups. The effect of methyl groups on the phase assignment of *n*-alkane vibrations has been treated by several authors [122-124]. A modified version of the phase relationship has been derived [123,124], however, for all but the shortest *n*-alkanes this correction factor can be neglected. This analysis has not been extended to the longest wave length TA modes which in the *n*-alkane lattice correspond to librational motions about the two axes perpendicular to the chain axis. To investigate the effect of chain ends on the TA vibrations we have performed a lattice dynamical calculation on *n*-octane. Furthermore, we have repeated the *n*-octane calculations of Brunel and Dows [75] and Takeuchi et al. [73] in an attempt to resolve the discrepancies between these two calculations. We have used the force field listed in table 4 for methylene interactions and Schachtschneider's and Snyder's force field parameters [2] for the methyl groups. The conclusions are that we can duplicate the frequencies of both calculations but that two librational mode assignments have been reversed in the calculation of Brunel

and Dows [75]. The effect of including the linear term was found to be maximum for the long axis librational mode. The discrepancies between the two previous *n*-octane calculations arises from the reversal of two assignments.

We have compared the calculated lattice frequencies of *n*-octane with values generated from the theoretical dispersion curves of polyethylene. The results indicate that even for this short *n*-alkane there is excellent agreement between the frequencies and one is justified in using the *n*-alkane data to plot experimental skeletal dispersion curves of polyethylene.

TABLE 4. General force field parameters

No.	Type	Chemical Repeat Unit	Value[a]	σ
1	1,1	0	4.517	0.011
2	1,3	0	0.460	.066
3	1,4	0	0.143	.086
4	1,5	0	−0.096	.017
6	2,2	0	4.289	.023
7	2,7	0	−0.660	.043
8	3,3	0	4.187	.014
9	3,4	0	0.116	.033
10	3,5	0	−0.129	.057
11	3,6	0	−0.286	.003
13	4,4	0	1.005	.024
14	4,5	0	−0.010	.11
16	5,5	0	0.541	.011
18	6,6	0	0.582	.0028
20	7,7	0	0.8366	.021
21	8,8	0	0.624	.0045
22	9,9	0	0.085	.0043
23	1,4	1	0.0785	.0097
26	2,7	1	0.266	.011
27	3,3	1	0.065	.011
29	4,3	1	0.104	.012
30	4,4	1	0.123	.016
31	4,5	1	0.030	.097
32	4,6	1	−0.101	.0039
34	5,5	1	0.004	.0008
35	5,6	1	−0.012	.029
37	6,3	1	−0.004	.027
38	6,6	1	−0.037	.0013
40	7,7	1	−0.014	.0095
41	7,8	1	0.018	.0069
42	8,8	1	−0.066	.0013
43	9,9	1	−0.0074	.0088
45	4,4	2	0.005	.016
46	4,5	2	−0.014	.0026
47	4,6	2	0.048	.02
49	5,5	2	0.002	.03
51	7.7	2	0.0185	.003
52	9,9	2	0.0007	.0054

[a] The units are millidyne/Angstrom (10^2N·m^{-1}) for stretch-stretch terms; millidyne·Angstrom (10^{-18}N·m) for bend-bend terms; and millidynes (10^{-8}N) for stretch-bend terms.

Localized symmetry internal coordinates:

1. Symmetric C–H stretch.
2. Asymmetric C–H stretch.
3. Skeletal (CC) stretch.
4. Skeletal (CCC) angle bend.
5. Methylene scissors.
6. Methylene wag.
7. Methylene rock.
8. Methylene twist.
9. Skeletal torsion.

TABLE 5. Interatomic potential energy parameters
$V(r) = -ar^{-6} + be^{-cr}$

Type	a(mdyn Å^7)	b(mdyn Å)	c(Å^{-1})
H . . H	0.250	17.77	3.74
H . . . C	2.014	99.49	3.67
C . . . C	3.716	1036.4	3.60

Conclusions

A review of previous normal mode calculations has shown that the structural and force field models employed in these calculations do not adequately describe the recent low frequency vibrational data. We have used these frequencies together with structural and vibrational data obtained at similar temperatures to determine a valence force field and intermolecular potential energy function for polyethylene and the *n*-alkanes. The valence force field was described in terms of localized symmetry coordinates which facilitated the linear regression calculation by removing some of the correlation.

The parameters of an exponential–6 type potential energy function were refined to obtain the best agreement with experimental frequencies. Excellent agreement was obtained with the observed factor group splittings and zone center lattice modes. In particular, we have been able to fit the long axis librational mode frequencies of the triclinic and orthorhombic structures. The transverse acoustical frequencies calculated from our force field and nonbonded potential energy expression are too low in frequency. We

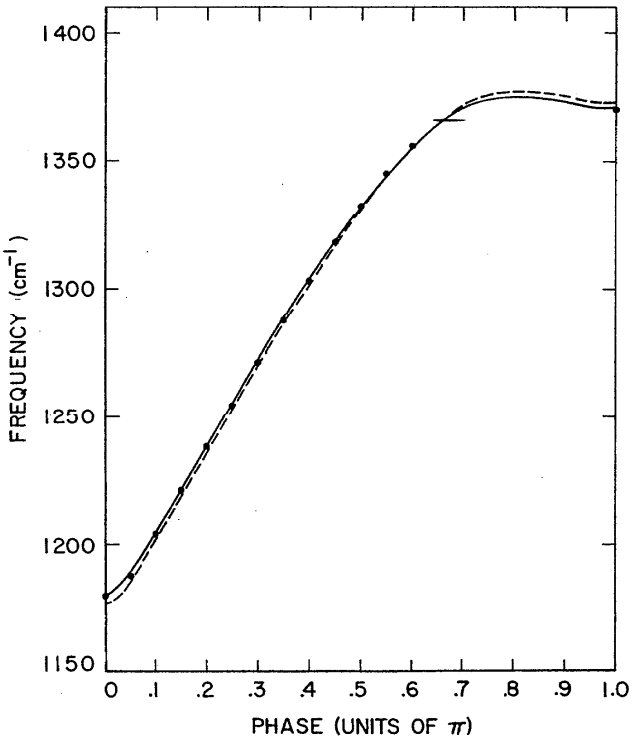

FIGURE 1. Experimental (dotted curve) and theoretical (dashed and solid curves) methylene wagging dispersion curves of the orthorhombic polyethylene lattice.

TABLE 6. Experimental and calculated frequencies of polyethylene (orthorhombic structure)

Symmetry	Calc. (cm^{-1})	Obs. (cm^{-1})	Assignment
A_g	Raman active		
	141.2	136	libration
	1137.5	1133	optical skeletal
	1175.2	1170	methylene rock
	1445.0	1442	methylene scissors
	2854.6	2848	symmetric C–H stretch
	2884.8	2883	asymmetric C–H stretch
A_u			
	54.9	inactive	translatory
	1040.6	inactive	methylene twist
	1180.8	inactive	methylene wag
B_{1g}	Raman active		
	1065.8	1065	optical skeletal
	1296.8	1297	methylene twist
	1370.7	1370	methylene wag
B_{1u}	Infrared active		
	0.0		
	85.9	81	translatory
	736.5	734	methylene rock
	1477.8	1473	methylene scissors
	2851.5	2851	symmetric C–H stretch
	2921.5	2919	asymmetric C–H stretch
B_{2g}	Raman active		
	1069.6	1068	optical skeletal
	1293.4	1295	methylene twist
	1373.2	1370	methylene wag
B_{2u}	Infrared active		
	0.0		
	109.1	106	translatory
	720.7	721	methylene rock
	1472.3	1463	methylene scissors
	2852.9	2851	symmetric C–H stretch
	2921.7	2919	asymmetric C–H stretch
B_{3g}	Raman active		
	101.5	108	libration
	1137.0	1133	optical skeletal
	1176.1	1170	methylene rock
	1458.3	1442	methylene scissors
	2849.9	2848	symmetric C–H stretch
	2888.7	2883	asymmetric C–H stretch
B_{3u}	Infrared active		
	0.0		
	1042.9	1050	methylene twist
	1177.3	1175	methylene wag

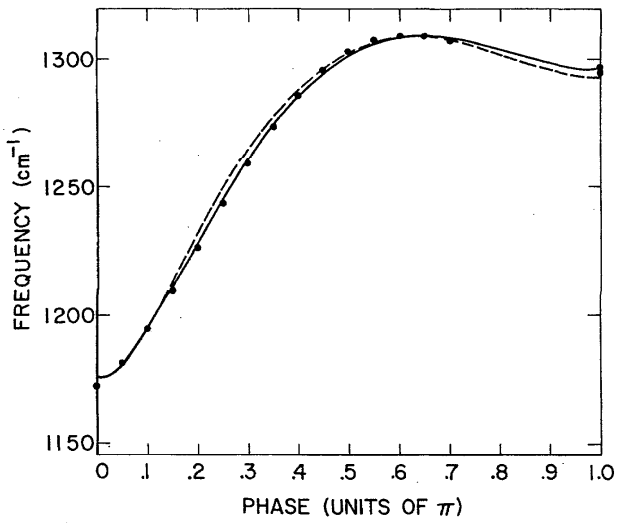

FIGURE 2. Experimental (dotted curve) and theoretical (solid and dashed curves) methylene twisting dispersion curves of the orthorhombic polyethylene lattice.

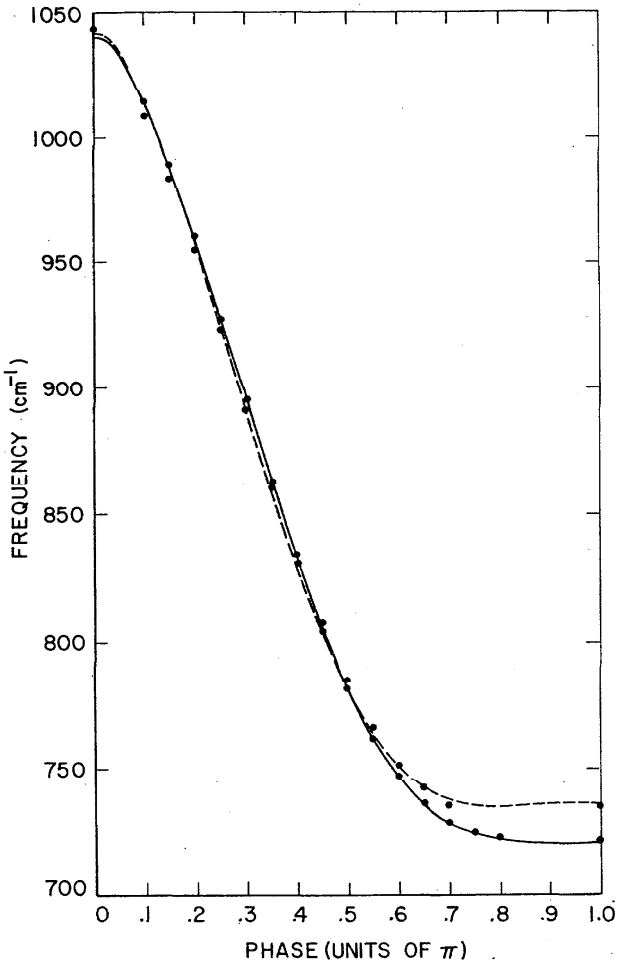

FIGURE 3. Experimental (dotted curves) and theoretical (solid and dashed curves) methylene rocking dispersion curves of the orthorhombic polyethylene lattice.

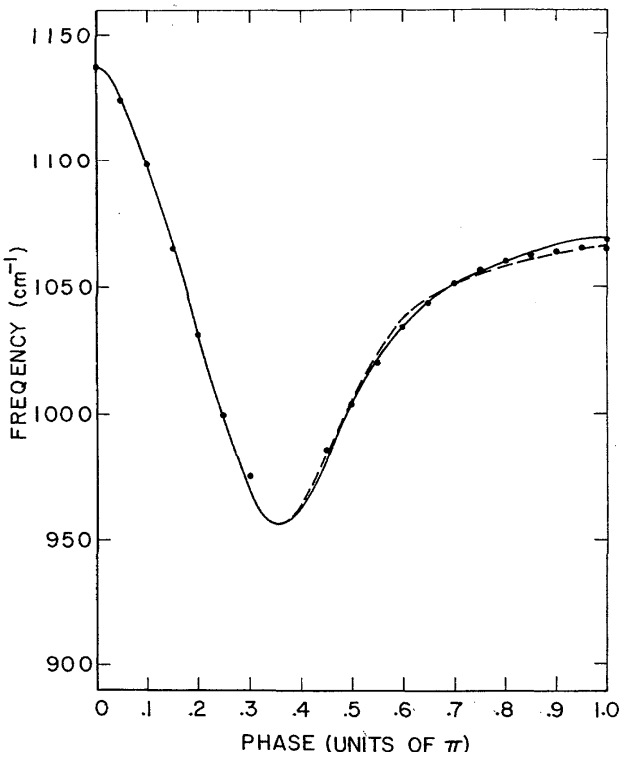

FIGURE 4. Experimental (dotted curve) and theoretical (solid and dashed curves) optical skeletal dispersion curves of the orthorhombic polyethylene lattice.

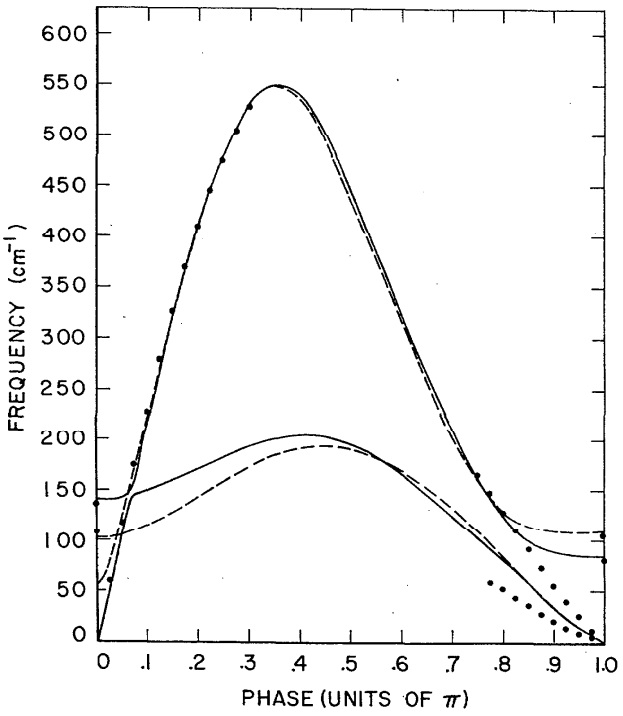

FIGURE 5. Experimental (dotted curves) and theoretical (solid and dashed curves) acoustical dispersion curves of the orthorhombic polyethylene lattice.

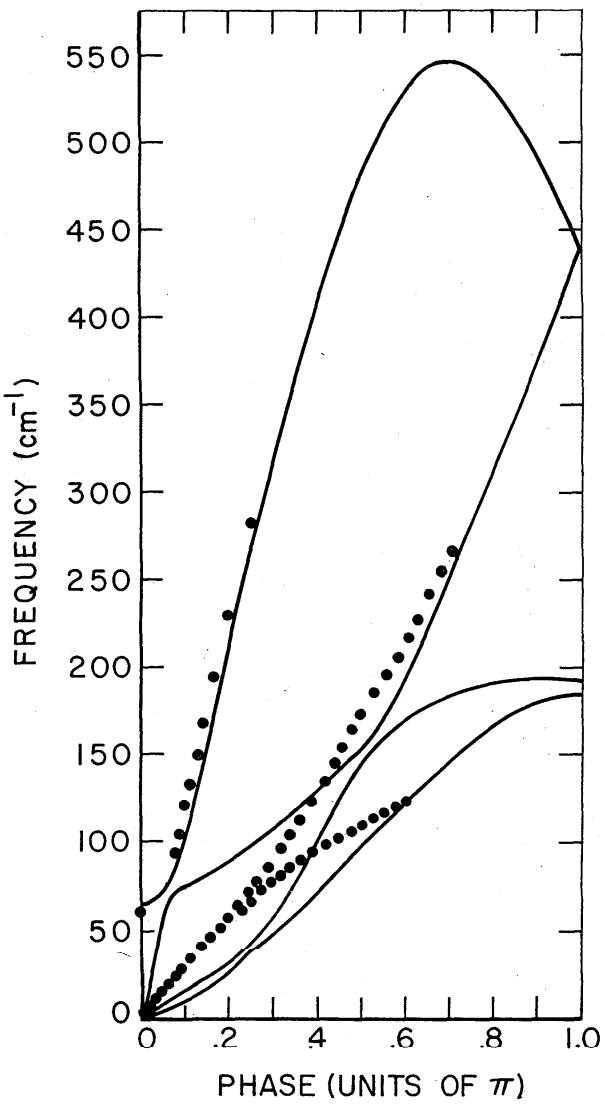

FIGURE 6. Experimental (dotted curves) and theoretical (solid curves) acoustic dispersion curves of the triclinic polyethylene lattice.

have not been able to reconcile the difference within the confines of our model. It has been suggested [125] that a coulombic interaction term arising from residual effective charges be included or that anharmonicity may play the dominant role.

References

[1] Snyder, R. G., and Schachtschneider, J. H., Spectrochim. Acta **19**, 85 (1963).
[2] Schachtschneider, J. H., and Snyder R. G., Spectrochim. Acta **19**, 117 (1963).
[3] Bunn, C. W., Trans. Faraday Soc. **35**, 482 (1939).
[4] Bunn, C. W., and Alcock, T. C., Trans. Faraday Soc. **41**, 317 (1945).
[5] Kavesh, S., and Schultz, J. M., J. Poly. Sci. Part A-2, **8**, 243 (1970).
[6] Wunderlich, B., Macromolecular Physics, 1, *Crystal Structure, Morphology, Defects*, Academic Press, New York, 1973.
[7] Matthews, J. L., Peiser, H. S., and Richards, R. B., Acta Cryst. **2**, 85 (1949).
[8] Krimm, S., and Tobolsky, A. V., J. Polym. Sci. **7**, 57 (1951).
[9] Hermans, P. H., and Weidinger, A., Makromol. Chem. **44-46**, 24 (1961): **50**, 98 (1961).
[10] Martuscelli, E., and Martynov, M. A., Makromol. Chem. **111**, 50 (1968).
[11] Miller, R. G. J., and Willis, H. A., J. Polym. Sci. **19**, 485 (1956).
[12] Okada, T., and Mandelkern, L., J. Polym. Sci. (A-2) **5**, 239 (1967).
[13] Read, B. E., and Stein, R. S., Macromolecules **1**, 116 (1968).
[14] Zerbi, G., Piseri, L., and Cabassi, F., Mol. Phys. **22**, 241 (1971).
[15] Smith, A. E., J. Chem. Phys. **21**, 2229 (1954).
[16] Shearer, H. M. M., and Vand, V., Acta Cryst. **9**, 379 (1956).
[17] Vainstein, B. K., Lobachev, A. N., and Stasova, M. M., Soviet Phys. Cryst. **3**, 452 (1958).
[18] Teare, P. W., Acta Cryst. **12**, 294 (1959).
[19] Norman, N., and Mathisen, H. Acta. Chem. Scand. **15**, 1747 (1961).
[20] Norman, N., and Mathisen, H., Acta Chem. Scand. **15**, 1755 (1961).
[21] Mathisen, H., Norman, N., and Pedersen, B. F., Acta Chem. Scand. **21**, 127 (1967).
[22] Nyburg, S. C., and Luth, H. Acta Cryst. **B-28**, 2992 (1972).
[23] Charlesby, A., Proc. Phys. Soc. **57**, 510 (1945).
[24] Walter, E. R., and Reding, F. P., J. Polym. Sci. **21**, 561 (1956).
[25] Sella, C., Compt. rend **248**, 2348 (1959).
[26] Cole, E. A, and Holmes, D. R., J. Polym. Sci. **46**, 245 (1960).
[27] Swan, P. R., J. Polym. Sci. **56**, 403 (1962).
[28] Aoki, Y., Chiba, A., and Kaneko, M., J. Phys. Soc. of Japan **27**, 1579 (1969).
[29] Avitabile, G., Napolitano, R., Pirozzi, B., Rouse, K. D., Thomas, M. W., and Willis, B. T. M., J. Polym. Sci. Polym. Letr. Ed. **13**, 351 (1975).
[30] Snyder, R. G., J. Mol. Spectry. **7**, 116 (1961).
[31] Broadhurst, M. G., J. Res. Natl. Bur. Stand. (U.S.) **A66**, 241 (1962).
[32] Ohlberg, S. M., J. Phys. Chem. **63**, 248 (1959).
[33] Muller, A., Proc. Roy. Soc. (London) **A138**, 514 (1932).
[34] Andrew, E. R., J. Chem. Phys. **18**, 607 (1950).
[35] Olf, H. G., and Peterlin, A., J. Polym. Sci. A-2 **8**, 791 (1970).
[36] Barnes, J. D., and Fanconi, B., J. Chem. Phys. **56**, 5190 (1972).
[37] Barnes, J. D., J. Chem. Phys. **58**, 5193 (1973).
[38] Nielson, J. R., and Hathaway, C. E., J. Mol. Spectry. **10**, 366 (1963).
[39] Snyder, R. G., J. Mol. Spectry. **4**, 411 (1960).
[40] Nielson, J. R., and Holland, R. F., J. Mol. Spectry. **4**, 488 (1960).
[41] Nielsen, J. R., and Holland, R. F., J. Mol. Spectry. **6**, 394 (1961).
[42] Holland, R. F., and Nielsen, J. R., J. Mol. Spectry. **8**, 383 (1962).
[43] Willis, H. A., Miller, R. G., Adams, D. M., and Gebbie, H. A., Spectrochim. Acta **19**, 1457 (1963).
[44] Bertie, J. E., and Whalley, E., J. Chem. Phys. **41**, 575 (1964).
[45] Frenzel, A. O., and Butler, J. P., J. Opt. Soc. Am. **54**, 1059 (1964).
[46] McKnight, R. V., and Moller, K. D., J Opt. Soc. Am. **54**, 132 (1964).
[47] Krimm, S., and Bank, M., J. Chem. Phys. **42**, 4059 (1965).
[48] Dean, G. D., and Martin, D. H., Chem. Phys. Ltrs. **1**, 415 (1967).
[49] Bank, M. I., and Krimm, S., J. Appl. Phys. **39**, 4951 (1968).
[50] Shen, M., Hansen, N. N., and Romo, P. C., J. Chem. Phys. **51**, 425 (1969).
[51] Chantry, G. W., Fleming, J. J. W., Smith, P. M., Cudby, M., and Willis, H. A., Chem. Phys. Ltrs. **10**, 473 (1971).
[52] Amshein, E. M., and Heil, H., J. Phys. Chem. Solids **32**, 1925 (1971).
[53] Fleming, J. W., Chantry, G. W., Turner, P. A., Nicol, E. A., Willis, H. A., and Cudby, M. E. A., Chem. Phys. Lrs. **17**, 84 (1972).

[54] Davis, G. J., and Haigh, J., Infrared Physics **14**, 183 (1974).
[55] Mizushima, S., and Shimanouchi, T., J. Amer, Chem. Soc. **71**, 1320 (1949).
[56] Brown, R. G., J. Chem. Phys. **38**, 221 (1963).
[57] Schaufele, R. F., and Shimanouchi, T., J. Chem. Phys. **47**, 3605 (1967).
[58] Frenzel, C. A., Bradley, E. B., and Mathur, M. S., J. Chem. Phys. **49**, 3789 (1968).
[59] Hendra, P. A., J. Mol. Spectry. **28**, 118 (1968).
[60] Snyder, R. G., J. Mol. Spectry. **31**, 464 (1969).
[61] Boerio, F. J., and Koenig, J. Chem. Phys. **52**, 3425 (1970).
[62] Carter, V., Mol. Spectry. **36**, 222 (1970).
[63] Snyder, R. G., J. Mol. Spectry. **34**, 356 (1970).
[64] Gall, M. J., Hendra, P. J., Peacock, C. J., Cudby, M. E. A., and Willis, H. A., Polymer **13**, 104 (1972).
[65] Gall, M. H., Hendra, P. J., Peacock, C. J. Cudby, M. E. A., and Willis, H. A., Spectrochim. Acta. **38A**, 1485 (1972).
[66] Fraser, G. V., Hendra, P. J., Cudby, M. E. A. and Willis, H. A., J. C. S. Chem. Comm. **16** (1973).
[67] Wu, C. K., and Nicol, M., J. Chem. Phys. **58**, 5150 (1973).
[68] Khoury, F., Fanconi, B., Barnes, J. D., and Bolz, L. H., J. Chem. Phys. **59**, 5849 (1973).
[69] Olf, H. G., and Fanconi, B., J. Chem. Phys. **59**, 534 (1973).
[70] Harley, R. T., Hayes, W., and Twisleton, J. F., J. Phys. C: Solid State Phys. **6**, L167 (1973).
[71] Vergoten, G., Fleury, G., Tasumi, M., and Shimanouchi, T., Chem. Phys. Letters **19**, 191 (1973).
[72] Wu, C. K., and Nicol, M., Chem. Phys. Letters **18**, 83 (1973).
[73] Takeuchi, H., Shimanouchi, T., and Tasumi, M., Chem. Phys. Letrs. **28**, 449 (1974).
[74] Wu, C. K., and Nicol, M., Chem. Phys. Letters. **24**, 395 (1974).
[75] Brunel, L. C., and Dows, D. A., Spectrochim. Acta **30A**, 929 (1974).
[76] Fanconi, B., J. Appl. Phys. **46**, 4124 (1975).
[77] Strobl, G. R., and Eckel, R., J. Polymer Sci. Polymer Physics Edition **14**, 913 (1976).
[78] Danner, H. R., Boutin, H., and Safford, G. J., J. Chem. Phys. **41**, 3649 (1964).
[79] Danner, H. R., Safford, G. J., Boutin, H., and Berger, M., J. Chem. Phys. **40**, 1417 (1964).
[80] Summerfield, G. C., J. Chem. Phys. **43**, 1079 (1965).
[81] Myers, W., Donavan, J. L., and King, J. S., J. Chem. Phys. **42**, 4299 (1965).
[82] Myers, W., Summerfield, G. C., and King, J. S., J. Chem. Phys. **44**, 184 (1966).
[83] Safford, G. J., Naumann, A. W., and Simon, F. T., J. Chem. Phys. **45**, 3787 (1966).
[84] Trevino, S., and Boutin, H., J. Macromol. Sci. Chem. A1, 723 (1967).
[85] Myers, W. D., and Randolph, P. D., J. Chem. Phys. **49**, 1043 (1968).
[86] Feldkamp, L. A., Vankataraman, G. and King, J. S., *Neutron Elastic Scattering*, Proceedings of a Symposium on Neutron Inelastic scattering held at Copenhagen, May 1968, Vol. II, p 159, IAEA: Vienna (1968).
[87] Berghmans, H, Safford, G. J., and Leung, P. S., J. Polym. Sci. Pt. A-2, **9**, 1219 (1971).
[88] Twisleton, J. F., and White, J. W., 3rd Int'l. Symp. Chem. Org. Solid State, p. 33 (1972).
[89] Logan, D. W., Danner, H. R., Gault, J. D., and Kim, H., J. Chem. Phys. **59**, 2305 (1973).
[90] Kitagawa, T., and Miyazawa, T., Bull, Chem. Soc. of Japan **43**, 372 (1970).
[91] Kitagawa, T., and Miyazawa, T., Bull. Chem. Soc. of Japan **42**, 3437 (1969).
[92] Snyder, R. G., J. Mol. Spectry. **23**, 224 (1967).
[93] Miyazawa, T., JAERI 1157, **19** (1968).
[94] Kitagawa, T., and Miyazawa, T., Adv. Polym. Sci. **9**, 335 (1972).
[95] Lynch, J. E., Doctoral Thesis, University of Michigan, 1968.
[96] Liang, C. Y., J. Mol. Spectry. **1**, 61 (1957).
[97] Tobin, M. C., J. Chem. Phys. **23**, 891 (1955).
[98] Snyder, R. G., J. Mol. Spectry. **4**, 411 (1960).
[99] Urey, H. C., and Bradley, C. A., Phys. Rev. **38**, 1969 (1931).
[100] Simanouti, T., J. Chem. Phys. **17**, 245, 848 (1949).
[101] Snyder, R. G., J. Chem. Phys. **47**, 1316 (1967).
[102] Zbinden, R., Infrared Spectroscopy of High Polymers (Academic Press, New York). 1964. Chapter III.
[103] Stein, R. S., and Sutherland, G. B. B. M., J. Chem. Phys. **22**, 1993 (1954).
[104] Stein, R. S., and Sutherland, G. B. B. M., J. Chem. Phys. **21**, 370 (1953).
[105] Stein, R. S., J. Chem. Phys. **23**, 734 (1955).
[106] Simanouti, T., J. Chem. Phys. **17**, 734 (1949).
[107] Tasumi, M., Shimanouchi, T., and Miyazawa, T., J. Mol. Spectry. **9**, 261 (1962).
[108] Piseri, L, and Zerbi, G., J. Chem. Phys. **48**, 3561 (1968).
[109] Lin, T. P., and Koenig, J. L., J. Mol. Spectry. **9**, 228 (1962).
[110] Tasumi, M., Shimanouchi, T., and Miyazawa, T., J. Mol. Spectry. **11**, 422 (1963).
[111] Enomoto, S., and Asahina, M., J. Polym. Sci. Pt. A2, 3523 (1964).
[112] Miyazawa, T., and Kitagawa, T., J. Polym. Sci. **B2**, 395 (1964).
[113] Kitagawa, T., and Miyazawa, T., J. Chem. Phys. **47**, 337 (1967).
[114] Shimanouchi, T., and Tasumi, M., Indian Journal of Pure and Applied Physics **9**, 958 (1971).
[115] Marsh, D. I., and Martin, D. H., J. Phys. C: Solid State Phys. **5**, 2309 (1972).
[116] Kitagawa, T., and Miyazawa, T., Polymer J. **1**, 471 (1970).
[117] Tasumi, M., and Shimanouchi, T., J. Chem. Phys. **43**, 1245 (1965).
[118] Tasumi, M., and Krimm, S., J. Chem. Phys. **46**, 755 (1967).
[119] Williams, D. E., J. Chem. Phys. **45**, 3770 (1966).
[120] Williams, D. E., J. Chem. Phys. **47**, 4680 (1967).
[121] Williams, D. E., Trans. Am. Crys. Assoc. **6**, 21 (1970).
[122] Szigeti, B., Proc. Roy. Soc. (London) **A264**, 198 (1961).
[123] Matsuda, H., Okada, K., Takase, T., and Yamamoto, T., J. Chem. Phys. **41**, 1527 (1964).
[124] Okada, K., J. Chem. Phys. **43**, 2497 (1965).
[125] Warshel, A., and Lifson, S., J. Chem. Phys. **53**, 583 (1970).